

# Internal charge-phosphor field characteristics of alternating-current thin-film electroluminescent devices

A. Abu-Dayah, S. Kobayashi, and J. F. Wager

Department of Electrical and Computer Engineering, Center for Advanced Materials Research, Oregon State University, Corvallis, Oregon 97331-3211

(Received 7 August 1992; accepted for publication 24 November 1992)

The internal charge versus phosphor field ( $Q$ - $F_p$ ) technique is proposed as a method for characterization of the electrical properties of alternating-current thin-film electroluminescent (ACTFEL) devices.  $Q$ - $F_p$  analysis provides direct information about the internal behavior of the ACTFEL device. The steady-state field and internal conduction, polarization, leakage, and relaxation charges may be readily deduced from a  $Q$ - $F_p$  plot.

The standard method used to characterize the electrical properties of alternating-current thin-film electroluminescent (ACTFEL) devices is the charge versus voltage ( $Q$ - $V$ ) technique.<sup>1-7</sup> The purpose of this letter is to propose a new approach for electrical characterization of ACTFEL devices, the internal charge versus phosphor field ( $Q$ - $F_p$ ) technique. The  $Q$ - $F_p$  technique displays the internal electrical characteristics of the ACTFEL device rather than a combination of internal and external characteristics as is the case for the  $Q$ - $V$  technique.<sup>7</sup>

$Q$ - $F_p$  analysis is accomplished using the circuit shown in Fig. 1. An arbitrary wave form generator (Wavetek model 275) provides a 1 kHz wave form of symmetric bipolar pulses with 5  $\mu$ s rise and fall times and a 30  $\mu$ s pulse width. A series resistor,  $R_s$ , of magnitude 200  $\Omega$  and a sense capacitor,  $C_s$ , 100 times larger than the total capacitance are placed in series with the ACTFEL device. Voltages  $v_1(t)$ ,  $v_2(t)$ , and  $v_3(t)$  are obtained by sampling using a Tektronix model 7854 digitizing oscilloscope.

The instantaneous charge in the phosphor,  $q(t)$ , is obtained from<sup>8</sup>

$$q(t) = \frac{C_i + C_p}{C_i} C_s v_3(t) - C_p [v_2(t) - v_3(t)], \quad (1)$$

where  $C_i$  and  $C_p$  are the insulator and phosphor capacitors, respectively. In the absence of space charge in the phosphor, the instantaneous electric field in the phosphor,  $F_p(t)$ , is given by<sup>8</sup>

$$F_p(t) = \frac{1}{d_p} \left( \frac{C_s v_3(t)}{C_i} - [v_2(t) - v_3(t)] \right), \quad (2)$$

where  $d_p$  is the phosphor thickness. A  $Q$ - $F_p$  curve is obtained by plotting  $q(t)$  versus  $F_p(t)$ , as assessed from Eqs. (1) and (2), respectively.

A  $Q$ - $F_p$  curve for an evaporated ZnS:Mn ACTFEL device with sputtered SiON insulators is shown in Fig. 2. The labels A through J are used to designate certain points on the  $Q$ - $F_p$  curve; these points are also shown on a corresponding  $Q$ - $V$  curve, as indicated in Fig. 3. Superscripts + and - used in Figs. 2 and 3 correspond to the polarity of the applied voltage pulse; a positive voltage pulse is defined as when the Al electrode bias is positive. Various fields and charges may be evaluated from the  $Q$ - $F_p$  curve as follows.  $F_{ss}$  corresponds to the steady-state phosphor

electric field concomitant with the emission of electrons from a large density of interface states.  $Q_{\text{cond}}$  is the conduction charge transported across the phosphor during the voltage pulse; this is the charge responsible for impact excitation of luminescent impurities and, hence, which gives rise to light emission.  $Q_{\text{pol}}$  is the polarization charge stored at the phosphor/insulator interface just prior to the onset of the subsequent pulse of opposite polarity. Note that  $Q_{\text{pol}}$  is identified with an "e" superscript in the  $Q$ - $V$  curve of Fig. 3 in order to distinguish this charge as an external charge; our convention is that the absence of such a superscript indicates the charge to be an internal charge. No "e" superscript is required in a  $Q$ - $F_p$  curve since all of the charges are internal.  $Q_{\text{leak}}$  denotes the leakage charge arising from the emission of electrons from shallow interface states<sup>7,9</sup> during the zero voltage portion of the wave form. Finally,  $Q_{\text{relax}}$  is the relaxation charge<sup>10,11</sup> which flows across the phosphor during the portion of the wave form at which the applied voltage is constant at its maximum value; the phosphor field relaxes during this period of the wave form, hence the identification as relaxation charge.

In order to further clarify the features of a  $Q$ - $F_p$  curve, a brief explanation of the curve from A to F is now provided. The point labeled A in Fig. 2 corresponds to the onset of a positive voltage pulse applied to the Al electrode. Nonzero values of  $Q$  and  $F_p$  are observed at A because of polarization charge residing at the phosphor/insulator interface left behind by the previous pulse of opposite polarity. The AB portion of the  $Q$ - $F_p$  curve arises from the rising edge of the external voltage when the magnitude is less than that required for turn-on of the ACTFEL device. BC also occurs during the rising portion of the external

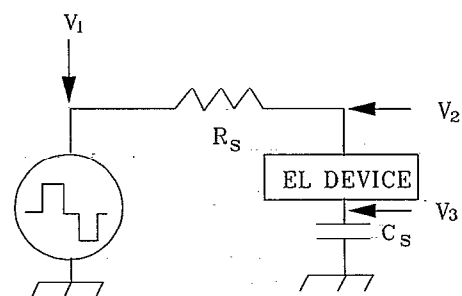


FIG. 1. Circuit used for  $Q$ - $F_p$  analysis.

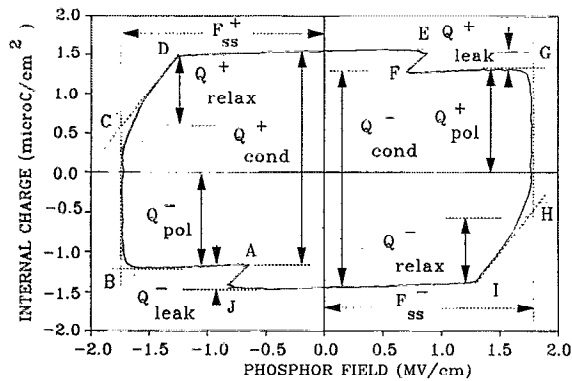


FIG. 2.  $Q$ - $F_p$  curve for an evaporated ZnS:Mn ACTFEL device with sputtered SiON dielectrics. The applied voltage amplitude is 240 V.

voltage pulse but the voltage magnitude is greater than the turn-on voltage for the BC portion of the  $Q$ - $F_p$  curve; the field is constant during much of this portion of the wave form and is equal to  $F_{ss}$ . CD corresponds to the portion of the wave form in which the external voltage is held constant at its maximum amplitude. Section DE of the  $Q$ - $F_p$  curve is obtained during the falling edge of the voltage pulse; the polarity of the phosphor field reverses during this portion of the wave form. EF corresponds to the segment of the wave form in which no external bias is applied to the ACTFEL device. The remainder of the  $Q$ - $F_p$  curve from F to A is similar to the A to F portion of the curve just described except that the external applied voltage pulse is of opposite polarity.

$Q$ - $F_p$  curves are compared in Fig. 4 and Table I between an evaporated ZnS:Mn ACTFEL device with sputtered SiON dielectrics and a ZnS:Mn ACTFEL device grown by atomic layer epitaxy (ALE) with aluminum-titanium-oxide (ATO) insulators. For comparison purposes the maximum applied voltage ( $V_{max}$ ) was chosen to be  $\sim 60$  V above threshold (i.e.,  $V_{max}=240$  V for evaporated and  $V_{max}=200$  V for ALE). There are several dramatic differences between these devices. First, much more conduction charge is transported across the phosphor in the ALE device; this is a simple consequence of the larger dielectric constant of ATO (i.e.,  $\approx 18.6$ ) compared to SiON ( $\approx 6.3$ ). Second  $Q_{leak}$  is much larger for the ALE

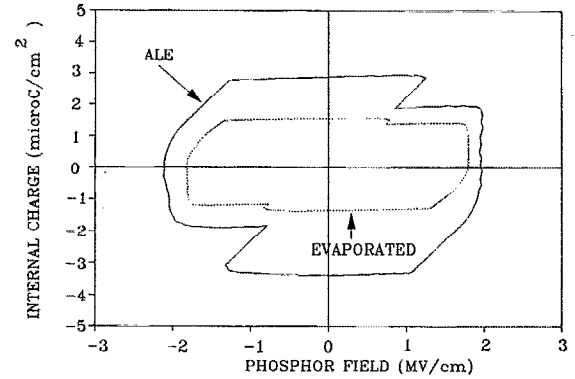


FIG. 4.  $Q$ - $F_p$  curves for an evaporated ZnS:Mn ACTFEL device with sputtered SiON dielectrics and an ALE ZnS:Mn device with ATO dielectrics. Both devices are operated at  $\sim 60$  V above threshold.

device and the fraction of leakage to conduction charge is also much greater in ALE devices compared to evaporated devices. Thus, much of the charge transported across the ALE phosphor appears to reside in relatively shallow traps such that it is easily emitted from these traps when the external bias is zeroed. Alternatively, the trap depths may be similar for the ALE and evaporated ACTFEL devices but these traps could be more readily emptied, and thus, contribute to the leakage charge, because of the large polarization field existing in the ALE device. Third, the evaporated ACTFEL device exhibits a distinct steady-state field. In contrast,  $F_{ss}$  in the ALE device is not well-defined and the magnitude and shape of the measured phosphor field depends on the polarity of the applied voltage pulse. For the ALE device, the positive voltage pulse exhibits a characteristic in which  $F_p$  increases and only reaches steady-state for a very small portion of BC; the negative voltage pulse displays a larger steady-state field regime but near G a field-overshoot region exists. Finally, note that the  $Q$ - $F_p$  characteristic is symmetric for the evaporated ACTFEL device but it is rather asymmetric for the ALE device.

A family of  $Q$ - $F_p$  curves is displayed as a function of  $V_{max}$  in Figs. 5 and 6 for an evaporated and ALE ACTFEL device, respectively. Note that strong field-clamping occurs in the evaporated device, since  $F_{ss}$  is independent of  $V_{max}$  whereas its absence is clearly evident in the ALE device. Also note in Fig. 6 near point G that the field-overshoot region is more pronounced at larger  $V_{max}$ 's.

We attribute the field-overshoot of the electrical char-

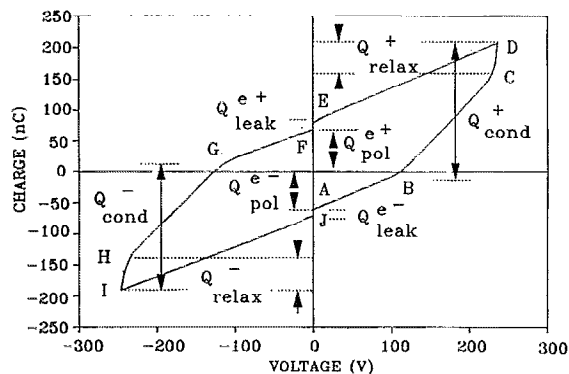


FIG. 3.  $Q$ - $V$  curve for an evaporated ZnS:Mn ACTFEL device with sputtered SiON dielectrics.

TABLE I. A comparison of various parameters measured from the  $Q$ - $F_p$  technique for an ALE and an evaporated ACTFEL device. + and - indicates the polarity of the voltage pulse applied to the Al electrode.

Measured parameter		ALE		Evaporated	
		+	-	+	-
$F_{ss}$	(MV/cm)	2.1	2.0	1.7	1.7
$Q_{leak}$	( $\mu C/cm^2$ )	1.0	1.6	0.3	0.3
$Q_{relax}$	( $\mu C/cm^2$ )	2.0	2.1	1.0	1.0
$Q_{cond}$	( $\mu C/cm^2$ )	4.7	5.3	2.8	2.8
$Q_{pol}$	( $\mu C/cm^2$ )	1.9	1.8	1.3	1.3

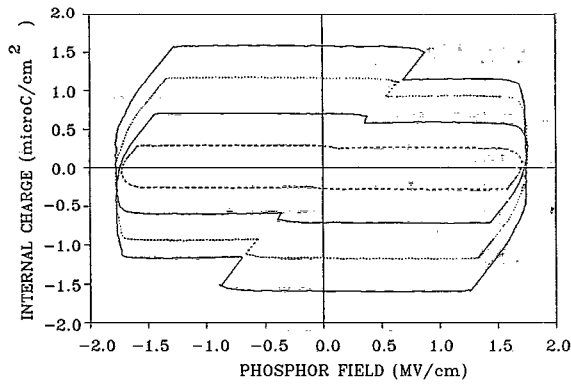


FIG. 5. A family of  $Q-F_p$  curves for an evaporated ZnS:Mn ACTFEL device with sputtered SiON dielectrics.  $V_{\max}$  = 180, 200, 220, and 240 V.

acteristics exhibited by ALE devices to the existence of space charge in the phosphor bulk.<sup>12,13</sup> Field-overshoot could also arise as a consequence of a certain distribution of interface states. We prefer to attribute field-overshoot to the presence of bulk space charge, because we find a capacitance-voltage ( $C-V$ ) overshoot to be concomitant with the  $Q-F_p$  overshoot and this  $C-V$  overshoot exhibits a capacitance peak well in excess of the insulator capacitance

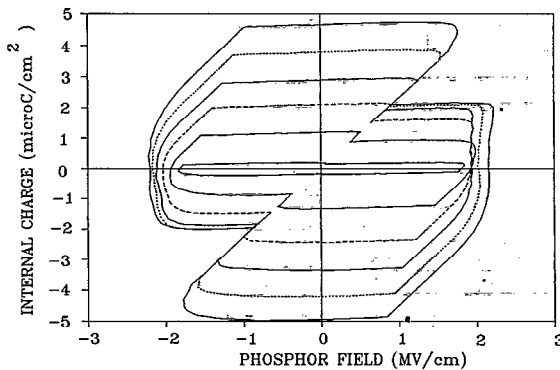


FIG. 6. A family of  $Q-F_p$  curves for an ALE ZnS:Mn ACTFEL device with ATO dielectrics.  $V_{\max}$  = 140, 160, 180, 200, 220, and 240 V.

which is inconsistent with the hypothesis that overshoot arises from interface states. Note that the existence of bulk space charge in the phosphor invalidates Eq. (2). However, the  $Q-F_p$  technique may still be gainfully employed if it is realized that  $F_p$  calculated from Eq. (2) is actually an effective phosphor field; care must be taken in interpreting such  $Q-F_p$  curves.

In the  $Q-F_p$  technique,  $F_p$  depends explicitly on  $C_i$  as indicated in Eq. (2). Thus, the accuracy of a  $Q-F_p$  curve depends upon how well  $C_i$  is established. We use  $C_i$  calculated from the known thickness and dielectric constants of the insulator layers. These calculated values for  $C_i$  are in good agreement with those measured by  $C-V$  analysis for evaporated ZnS:Mn ACTFEL devices, but do not always agree with those of ALE ZnS:Mn ACTFEL devices; the measured values of  $C_i$  for ALE devices tend to be greater than those calculated because of the absence of field-clamping and the existence of space charge in ALE devices.

In summary, we propose the  $Q-F_p$  technique as an alternative method of investigating the electrical properties of ACTFEL display devices.  $F_{ss}$ ,  $Q_{\text{cond}}$ ,  $Q_{\text{leak}}$ , and  $Q_{\text{relax}}$  may be readily assessed from a  $Q-F_p$  plot.

The authors wish to thank Ron Khormaei for providing the samples used in this study. This work was supported by the U. S. Army Research Office under Contract No. D11L03-91G0242.

<sup>1</sup>Y. S. Chen and D. C. Krupka, J. Appl. Phys. **43**, 4089 (1972).

<sup>2</sup>D. H. Smith, J. Lumin. **23**, 209 (1981).

<sup>3</sup>R. Mach and G. O. Müller, Phys. Status Solidi A **69**, 11 (1982).

<sup>4</sup>P. M. Alt, Proc. SID **25**, 123 (1984).

<sup>5</sup>R. Mach and G. O. Müller, Phys. Status Solidi A **81**, 609 (1989).

<sup>6</sup>Y. A. Ono, H. Kawakami, M. Fuyama, and K. Onisawa, Jpn. J. Appl. Phys. **26**, 1482 (1987).

<sup>7</sup>J. F. Wager, A. A. Douglas, and D. C. Morton, *Electroluminescence*, edited by V. P. Singh and J. C. McClure (Cinco Puntos, El Paso, TX, 1992), p. 92.

<sup>8</sup>E. Bringuier, J. Appl. Phys. **66**, 1316 (1989).

<sup>9</sup>S. Kobayashi, A. Abu-Dayah, and F. J. Wager, in Ref. 7, p. 234.

<sup>10</sup>A. A. Douglas and J. F. Wager, in Ref. 7, p. 387.

<sup>11</sup>A. A. Douglas and J. F. Wager, SID92 Digest, 356 (1992).

<sup>12</sup>A. Geoffroy and E. Bringuier, Semicond. Sci. Technol. **6**, A131 (1991).

<sup>13</sup>E. Bringuier and A. Geoffroy, Appl. Phys. Lett. **60**, 1256 (1992).